*All the authors of this manuscript declare that there is no conflict of interests regarding the publication of this article.

Research Article

Research on the Fault-Tolerant Federated Filtering Algorithm based on Wavelet Singular Value Detection

Jianhua Cheng,[1,2] Daidai Chen,[1] Rene Jr.Landry,[2] Lin Zhao,[1] Dongxue Guan[1]

[1] *Marine Navigation Research Institute, College of Automation, Harbin Engineering University, Harbin 150001, China*

[2] *LASSENA Laboratory, Ecole de Technologie Superieure, 1100 Notre-Dame Street West, Montreal, Quebec, H3C 1K3 Canada*

Correspondence should be addressed to Daidai Chen; ins_dai@hotmail.com

For the detection for soft fault in sensors, most fault detection methods applied in fault-tolerant federated filtering algorithm are insensitive, large-delay, and disabled to distinguish the fault types. To solve the problems above, a modulus maxima principle based fault detection method for navigation sensor is proposed in this paper. The relation between Lipschitz exponent and signal singularities has been established to detect and classify the sensor faults. By calculating the Lipschitz exponent at the fault point, the fault type of sensor can be distinguished, providing effective information for sensor fault isolation and restoration. It is especially effective to detect the step error and slope error in navigation sensors. Then, the algorithm based on wavelet singular value has been proposed to detect faults, which is applied to the federated filter for the INS/GPS/DVL integrated navigation system Simulation is conducted and its result shows that, this intelligent federated filter algorithm can accurately realize sensor fault detection and system reconstruction.

1. Introduction

With the development of modern ships, aircraft, missiles and other vehicles, ever higher standards for the accuracy and reliability of navigation systems are demanded. Because of the outstanding characters such as high-accuracy, self-contained and jam-proof, the inertial navigation system (INS) has become the core of navigation systems for most vehicles. Moreover, because the navigation errors in satellite navigation system and Doppler system don't accumulate, they have been the best external auxiliary navigation methods for calibrating INS and inhibiting the error accumulation all the time [1].

The performance of satellite positioning and Doppler velocity log can affect the calibration accuracy of INS directly. However, satellite positioning and Doppler velocity log are the navigation technology without autonomy. And so, not only the equipment errors but also the external environment disturbance will have harmful effects on them producing fault information, such as step error caused by clock jumping, power fluctuation in satellite positioning, and slope error caused by clock drift and the inaccuracy of rail parameter model [2]. Therefore, in order to improve the performance and reliability of navigation system, developing a fault-tolerant technology to detect and isolate system fault timely is very significant for engineering application.

Since the early 1970s, pioneer researchers have been studing on the projects related to fault detection for dynamic system. Among the fault detection methods for sensors, state χ^2 detection method based on Kalman filtering, residual χ^2 detection method and sensor fault detection based on modulated Gaussian wavelet transformation are correspondingly developed up to now. χ^2 detection method judge whether faults occur in the system by testing if the mean and variance of the constructed n dimensions Gaussian distribution random variables correspond to the assumptive values, and so this method is easy to calculate and understand practically. Utilizing the good local characteristic of modulated Gaussian wavelet, the fault detection method based on Gaussian wavelet transformation can effectively detect faults by adjusting the scaling factor. However, the methods mentioned above still have problems in common:

(1) It is insensitive and large-delay to detect soft faults, which is discussed in reference [3] and [4];

(2) Setting a certain threshold value to the designed function of fault detection, traditional fault detection can be used for knowing if faults occur, but the fault type can not be distinguished5].

To solve the problems above, a fault-tolerant federated filtering algorithm based on wavelet modulus maxima is proposed. The algorithm has high sensitivity to soft fault of navigation sensors, and can judge the fault type according to the Lipschitz exponent at the fault point.

2. Design for fault-tolerant filtering scheme

IThe malfunction in navigation subsystem will make the entire system lose effectiveness, and it is very difficult to positioning specific fault for complex systems. Focusing on the problems above, decentralized filter method is adopted for INS/GPS/DVL integrated navigation system, and fault detection is applied to the two sub filters, respectively. The overall design of fault tolerant system based on federated filter is shown as figure 1.

As shown in the figure 1, position measurement information Z_{IG} is the difference value between GPS and INS output, and velocity measurement information Z_{ID} is the difference value between DVL and INS output. Next, wavelet fault detection is carried out for Z_{IG} and Z_{ID}. When on faults are detected, measurement information Z_{IG} and Z_{ID} can be used for sub filter 1 and filter 2. Otherwise, the system will prevent the measurement information Z_{IG} and Z_{ID} from being sensor input signal, and the fault will be corrected according to the information provided by fault detector. When part of the navigation sensor fault occurs, the design shown as Figure 1 enables the integrated navigation system to work normally. That is to say, fault signal will have no effect on system output information, improving the fault tolerance of the system. Therefore, the key for designing the fault-tolerance filter

approach is detecting the state of external navigation information timely and accurately, to provide the optimal navigation information for the system calibration.

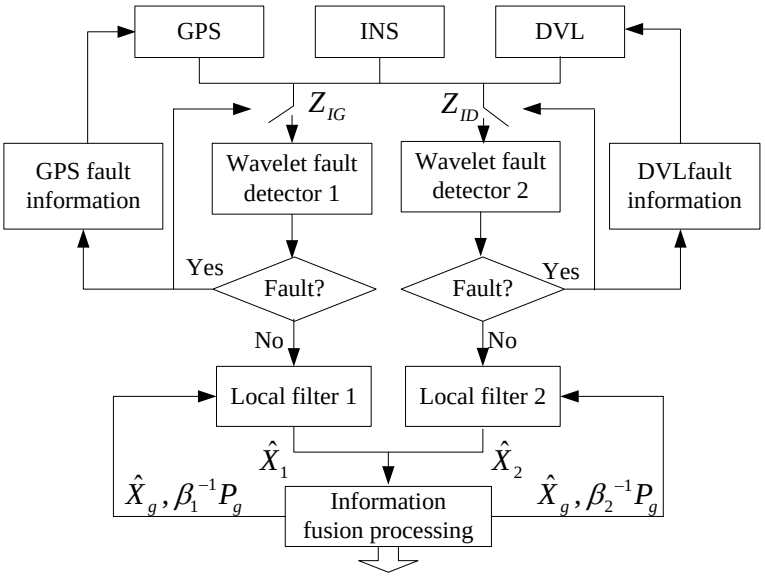

Figure.1 Integrated navigation design based on fault-tolerant federated filter

3. Signal singularity detection based on wavelet modulus maxima

3.1 Modulus maxima of wavelet transform

Signal f is processed by continuous wavelet transform, and there are several definitions on the scale s_0:

(1) If the derivative of the wavelet transformation coefficient $W_f(s_0,u)$ with respect to u equals to zero at the point $u=u_0$, there is a local extremum in wavelet transformation.

(2) If $W_f(s_0,u) \le W_f(s_0,u_0)$ is true for any point u within the neighbourhood of u_0 and inequality relation $W_f(s_0,u) < W_f(s_0,u_0)$ is satisfied strictly in the left or right neighborhood, point (s_0,u_0) is the maximum point of the wavelet transformation modulus $W_f(s,u)$ on the scale s_0, and $|W_f(s_0,u_0)|$ is the modulus maxima for the wavelet transform.

(3) If every point of a curve in the plane (s,u) is the maximum value of wavelet transformation coefficient $|W_f(s,u)|$, the curve is defined as the maximum curve.

Some important local information of signals can be inferred by the modulus maxima of the wavelet transform. By searching the modulus maxima, the modulus maxima curve on the different scales can be obtained, and then we can know the local singularities of signal through the change of the wavelet modulus maxima on different scales.

3.2 Relationship between modulus maxima and signal singularity

Assuming that $\psi(t) \in L^1(\mathbf{R}) \cap L^2(\mathbf{R})$ represents the square integrable real space, its Fourier transform $\hat{\psi}(\omega)$ meets the following condition[7]:

$$c_\psi = \int_{-\infty}^{+\infty} \frac{|\hat{\psi}(\omega)|^2}{|\omega|} \mathrm{d}\omega < +\infty \tag{1}$$

Where, the $\psi(t)$ is admissible wavelet or mother wavelet, and the equation (1) is the wavelet admissible condition. After the dilation and translation for the mother wavelet, we can get:

$$\psi_{s,u}(t)=\frac{1}{\sqrt{|s|}}\psi\left(\frac{t-u}{s}\right)\quad s,u\in \mathrm{R}, s\neq 0 \tag{2}$$

Where, s is scale factor; and u is translation factor. With the decrease of $|s|$, the wavelet function locality and time-domain resolution are improved, and frequency resolution is reduced. Conversely, with the increase of $|s|$, the wavelet function locality and time-domain resolution are reduced, and frequency resolution is improved.

Assuming that $\theta(t)$ is a smooth function, wavelet $\psi(t)$ and the signal f to be analyzed are both real function, scale parameter $s>0$, wavelet $\psi(t)$ is the first-order derivative of $\theta(t)$, then the continuous wavelet transform for f can be calculated easily:

$$W_f(s,u)=s^{1/2}(f*\bar{\psi}_s)(u)=s^{1/2}\frac{\mathrm{d}}{\mathrm{d}u}(f*\bar{\theta}_s)(u) \tag{3}$$

Where "*" represents the convolution operation, and $\bar{\theta}_s$ is the complex conjugate of θ_s.

From the equation (3), we can learn that wavelet transform modulus maxima is the maxima of the function f polished by $\bar{\theta}_s$, which accord with the breaking points of signal f as shown as Figure 2.

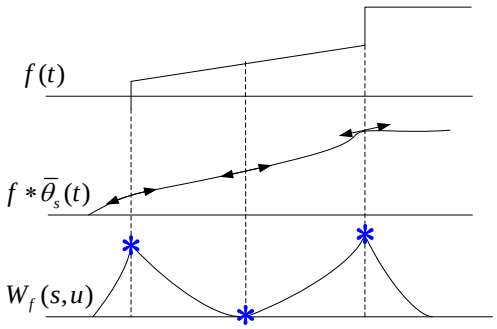

Figure.2 Signal breaking point based on wavelet modulus maxima detection

3.3 Simulation analysis for fault detection

Since there is no difficulty in detecting the step error, the slope error is set to verify the performance of the fault-detection method.

(1) Simulation conditions:

During 100~200s, the slope error is added to the output signal of navigation sensors.

(2) Simulation results:

The fault detection method based on Gaussian wavelet transform and the method based on wavelet modulus maxima proposed in reference [9] are applied to detecting faults respectively, and the Figure 3 and Figure 4 give the two fault detection results.

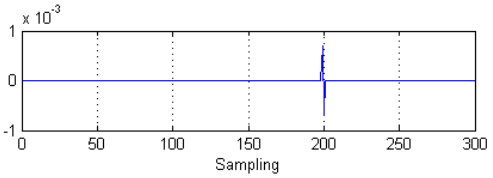

Figure.3 Slope fault detection based on Gaussian wavelet transform

Figure 3 shows that, there is hysteresis quality for fault detection using the algorithm based on Gaussian wavelet transform. That is to say, only the soft faults accumulate to certain degree, the faults can be detected.

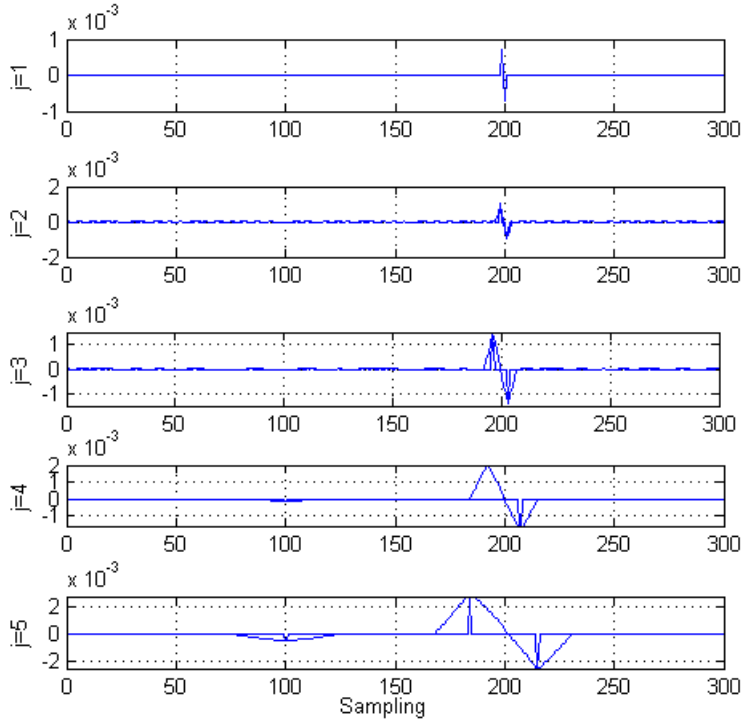

Figure.4 Slope fault detection by multi-scale transformation

From Figure 4, it can be seen that the signal time-domain resolution and the fault positioning accuracy are relatively high on small scales. However, with the increase of the decomposition scale, the signal has multiple extremum points caused by noise, and some of them decrease sharply or disappear. In all scales, the extreme values, which will not decrease with the increase of the scale, are the singularities of the signal itself. Aiming at the uncertainty of process and measurement noise statistic properties, the measurement information are used to real-time estimate and update the means and covariances of noises.

4. Fault type detection based on Lipschitz exponent

4.1 Lipschitz exponent characteristic of signal

Mathematically, the signal singularity is described by Lipschitz exponent[8]:

Definition 1: Assuming $f(t) \in L^2(\mathrm{R})$, if there are two constants M, $h_0(M>0, h_0>0)$ and n polynomial $g_n(h)$, making the following inequation true when $h < h_0$,

$$|f(h_0+h)-g_n(h_0)| \le M|h|^{\alpha} \tag{4}$$

The Lipschitz exponent of $f(x)$ at h_0 point is α.

For any point h_0, the polynomial $g_n(h)$ is uniquely determined. If $f(x)$ is $n=\lfloor \alpha \rfloor$ order continuously differentiable at h_0 point and its some neighborhood, the $g_n(h)$ is Taylor expansion of $f(x)$ at h_0 point. If function $f(x)$ has uniform Lipschitz exponent ($\alpha < n$) in some neighborhood of h_0 point, $f(x)$ is n order differentiable in this neighborhood. Therefore, the larger Lipschitz exponent α is, the better smoothness of $f(x)$ is; the smaller α is, the larger singularity of $f(x)$ is.

If $f(x)$ is first-order step function, considering:

$$|f(h_0+h)-g_n(h_0)| \le O|h|^0$$

According to equation (4), the Lipschitz exponent of step function at h_0 point is 0.

If $f(x)$ is first-order function, considering:

$$| f(h_0+h)-g_n(h_0) | \le O|h|$$

According to equation (4), the Lipschitz exponent of step function at h_0 point equals to 1.

The Lipschitz exponent related to random noise is usually less than zero. If Gaussian white noise is a random distribution which is singular almost everywhere, it has negative Lipschitz exponent $\alpha = -0.5-\varepsilon$, $\forall \varepsilon > 0$.

The relationship among the Lipschitz exponent of the three functions at the breaking point h_0 can be observed intuitively. The smoothness of step function is worse than function, and the smoothness of Gaussian white noise is worse than step function. According to the analysis above, the signal Lipschitz exponent α characteristics are summarized as follows:

(1) If $\alpha \ge 1$, function is derivable at x_0 point and function is first-order derivable at x_0 point when $\alpha = 1$; α value is directly proportional to the smoothness of signal;

(2) If $0 < \alpha < 1$, function is discontinuous at x_0 point, but the extreme value is limited;

(3) If $\alpha = 0$, the step of step function occurs at x_0 point;

(4) If $\alpha < 0$ and the distribution density decreases with the increase of the decomposition level wavelet transform, the signal can be affected by random noise.

4.2 Calculation of signal Lipschitz exponent based on modulus maxima

By analyzing the relationship between wavelet modulus of maxima transform and function singularity, Mallat and other scholars found that the attenuation of $|Wf(s,u)|$ could be controlled by its local maximum value. Therefore, the calculation of signal Lipschitz exponent can be completed by describing the relationship between wavelet modulus maxima and signal Lipschitz10].

Assume that the compactly supported set of wavelet function ψ is $[-C,C]$ ($C>0$), and all the modulus maxima points which converge to v point are in the conical surface $|u-v| \le Cs$ as shown in Figure 5, when $s < s_0$ is true.

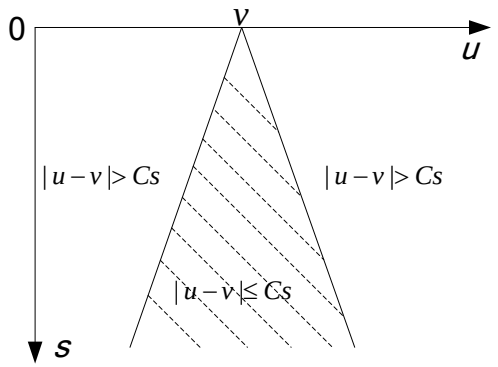

Fig.5 The conical surface composed of modulus maxima points

When function $f(t) \in L^2(\mathrm{R})$, the modulus maximum values distribute as the conical surface above, and point t_0 is Lipschitz($\alpha \le n$), there is the constant A that satisfy the following expression:

$$\forall (s,u) \in \mathrm{R}^+ \times \mathrm{R}, \left|W_f(s,u)\right| \le Aa^{\alpha+0.5} \cdot \left|1+\left|\frac{t-t_0}{s}\right|^{\alpha}\right| \tag{5}$$

When $t = t_0$, we can get:

$$\left|W_f(s,u)\right| \le Aa^{\alpha+0.5} \tag{6}$$

Evaluating the logarithm of the both sides in equation (6), and using binary wavelet transform, we can obtain the following comparison expression when $a = 2^j$:

$$\log_2 |W_f(a,b)| \le \log_2 A + j(\alpha + 0.5) \tag{7}$$

Equation (7) shows that, the Lipschitz exponent at t_0 point of function $f(t)$ depends on the attenuation of $|W_f(a,b)|$ under fine scales, that is to say,

(1) If $t = t_0$ and Lipschitz exponent $\alpha > 0$ are true, the wavelet transform modulus maxima is proportional to scale;

(2) If $t = t_0$ and Lipschitz exponent $\alpha < 0$ are true, the wavelet transform modulus maxima is inversely proportional to scale;

(3) If $t = t_0$ and Lipschitz exponent $\alpha = 0$ are true, the wavelet transform modulus maxima is not affected by scale.

Assuming that both sides of the comparison expression (7) are equal under the two continuous decomposition scale j and $j+1$[11], and then we can get:

$$\alpha = \frac{\log_2 \left|W_f(2^{j+1}, t_{j+1})\right| - \log_2 \left|W_f(2^j, t_j)\right|}{j+1-j} - 0.5 \tag{8}$$

According to equation (7) and (8), we know that $\log_2 |W_f(a,b)|$ as the function of decomposition scale j, equals to the result of substracting 0.5 from the slope of $\log_2 |W_f(a,b)|$ along the modulus maxima which converges to t_0. Equation (8) provides a more practical method to calculate the Lipschitz exponent.

4.3 Simulation and analysis for fault type detection

Driven by the slope faults mentioned in section 3.3, the signal has the attenuation relationship with the logarithm of modulus maxima at $u = 100$ and $u = 200$ point on scale j, and the relation curves are provided by Figure 6.

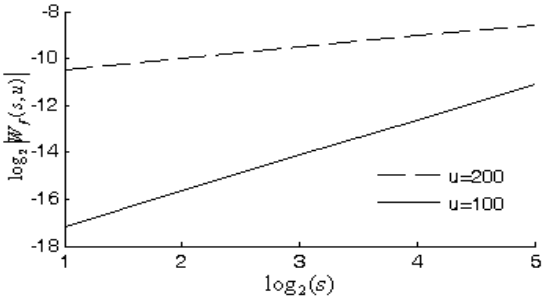

Figure.6 Slope of modulus maxima curve with slope fault

In Figure 6, the slopes at the two breaking points are relatively different, which is caused by the difference of the signal Lipschitz exponent at the two breaking points.

By using linear least square method, the slope of curve in figuer.6 at the modulus maxima on every scale of the curve can be estimated, and the Lipschitz exponent can be obtained by subtracting 0.5 from the slope. Under the two fault conditions, the scope of modulus maxima curve and Lipschitz exponent are shown as Table 1.

Table 1 Comparison of Lipschitz exponent

	Slope fault Lipschitz exponent	
Fault point	u=100	u=200
Modulus maxima curve slope	1.5143	0.4737
Measured value of α	1.0143	-0.0263
theoretical value of α	1	0

According to Table 1, there is approximately a superposition of firs-order derivable function at point $u=100$, and so α theoretical value can be approximated to 1; the step of step function occurs at point $u=200$, and so α theoretical value can be approximated to 0; the Lipschitz α exponent calculated by modulus maxima curve slope is basically the same with its theoretical value.

In conclusion, by using the good locality of Gaussian function, the fault detection based on Gaussian wavelet transform can mathematically magnify the signal singularity, but because the change of early signal in slope faults is not obvious, it is difficult to detect fault through modulated Gaussian wavelet transform. On the other hand, by searching wavelet modulus maxima on different scale, the fault detection method based on modulus maxima can find fault points, and the fault type can be distinguished through signal Lipschitz exponent calculated by the attenuation of wavelet modulus maxima.

5. Implement of fault detection algorithms

To obtain the singularity of fault signal and estimate Lipschitz exponent, we have to get the curves of modulus maxima. Theoretically, continuous wavelet transform should be carried out for signal processing, but because of the heavy computation burden, it can not be implemented in practical applications. Therefore, adhoc algorithm [12], which is the binary discrete wavelet transform with 2^j scale and continuous shift factor, is applied to finding the curves of modulus maxima. The fault detection algorithm can realize the functions, such as locating the faults, distinguishing fault type by Lipschitz exponent, and providing more effective information for fault isolation. The specific steps of the algorithm are shown as follows:

(1) Choosing Morlet wavelet basis and decomposition scale 2^j, we process the noise signal by binary discrete wavelet transform. With the decomposition scale chosen, the following requirements should be satisfied: The number of signal extreme points on the largest scale should be dominant; the important singularity of signal can not lost; the output signal delay can not affect on the real-time performance of integrated navigation system. According to the requirements above, we determine j=5 for the decomposition scale 2^j.

(2) Assuming that the largest amplitude of extreme point is M on largest decomposition scales, the extreme points whose amplitude is smaller than M/j should be eliminated, that is because the extreme points are caused by noise.

(3) For every extreme point x_0 on scale 2^j, assuming that the extreme value points before and after x_0 are x_1 and x_2 and the corresponding manifoldpoint of x_1 is x_1', so the corresponding manifoldpoint of x_0 should be found in the interval $L=[\max(x_1,x_1'),x_2]$; For the points $(a_1,a_2,\cdots a_n)$ which have the same sign with x_0 in the interval L, If $|a_k-x_0|\leq|a_i-x_0|/3, i=1,2,\cdots n, k\neq i$ is true, a_k is the manifoldpoint of x_0, else the point whose amplitude is the largest and sign is the same with x_0 is the manifoldpoint of x_0; If the amplitude of the manifoldpoint is double it of x_0, this point should be eliminated as the extreme value point of noise[13];

(4) Repeat the process above until the scale is 2^2;

(5) Eliminate the extreme point on the first scale 2^1, and put the distribution and amplitude of extreme point on the second scale 2^2 to the point on the first scale 2^1. The search for the modulus maxima on scale $2^j \sim 2^1$ is completed.

(6) Through the steps above, calculate the modulus maxima on every scale and draw the modulus maxima curve. According to the modulus maxima on fine scale, we can find the singular point position, namely the moment of fault occurrence.

(7) Select the modulus maxima point on every scale calculated in step (6) and the logarithm of decomposition scale as ordinate and abscissa respectively. The slope of curve is estimated by linear least squares, and Lipschitz exponent can be obtained by subtracting 0.5 from the curve slope. According to the LIpschitz exponent, we can distinguish the fault type, and the fault information is provided for fault detection and isolation module to dispose of the sensors with faults.

6. Fault-tolerant federated filter design

6.1 State and measurement equation for sub filter

Considering the outputs from the sensors are different from each other, indirect method is applied to estimate the navigation parameters. The state vector is selected as:

$$\boldsymbol{X}_I = [\delta\varphi \quad \delta\lambda \quad \delta V_x \quad \delta V_y \quad \alpha \quad \beta \quad \gamma \quad \varepsilon_x \quad \varepsilon_y \quad \varepsilon_z \quad \varepsilon_{rx} \quad \varepsilon_{ry} \quad \varepsilon_{rz}]^T$$

Where $\delta\varphi, \delta\lambda, \delta V_x, \delta V_y$ are the INS position errors and velocity errors; α, β, γ are attitude angel errors for INS; $\varepsilon_x, \varepsilon_y, \varepsilon_z$ are the constant gyro drifts; $\varepsilon_{\mathrm{rx}}, \varepsilon_{\mathrm{ry}}, \varepsilon_{\mathrm{rz}}$ are the random gyro drifts.

Position integrated mode is used for INS/GPS sub filter, so the state equation and measurement equation are given by:

$$\begin{bmatrix} \dot{\boldsymbol{X}}_I \\ \dot{\boldsymbol{X}}_G \end{bmatrix} = \begin{bmatrix} \boldsymbol{F}_I & \boldsymbol{0} \\ \boldsymbol{0} & \boldsymbol{F}_G \end{bmatrix} \begin{bmatrix} \boldsymbol{X}_I \\ \boldsymbol{X}_G \end{bmatrix} + \begin{bmatrix} \boldsymbol{W}_I \\ \boldsymbol{W}_G \end{bmatrix} \tag{9}$$

$$\boldsymbol{Z}_{IG} = \begin{bmatrix} \boldsymbol{\varphi}_I - \boldsymbol{\varphi}_G \\ \boldsymbol{\lambda}_I - \boldsymbol{\lambda}_G \end{bmatrix} = \boldsymbol{H}_{IG} \begin{bmatrix} \boldsymbol{X}_I \\ \boldsymbol{X}_G \end{bmatrix} + \boldsymbol{V}_{IG} \tag{10}$$

Where $\boldsymbol{F}_I$ is INS state transition matrix[14], $\boldsymbol{X}_G = [\delta\varphi_G \quad \delta\lambda_G]$ is the latitude error and longitude error. Using first order markov process to complete the approximate fitting, GPS state transition matrix $\boldsymbol{F}_G$ changes to be:

$$\boldsymbol{F}_G = \mathrm{diag}(\frac{1}{\tau_{\mathrm{GPS}\varphi}}, \frac{1}{\tau_{\mathrm{GPS}\lambda}}) \tag{11}$$

Where $\tau_{\mathrm{GPS}\varphi}$ and $\tau_{\mathrm{GPS}\lambda}$ are correlation time, $\boldsymbol{W}_{\mathrm{I}}, \boldsymbol{W}_{\mathrm{G}}$ are the system noise matrix for INS and GPS respectively, ω_{gx}, ω_{gy}, ω_{gz} are white noise caused by gyro drifts, $\omega_\varphi, \omega_\lambda$ are white noise caused by GPS, $\boldsymbol{V}_{IG}$ is measurement noise matrix, $\boldsymbol{H}_{IG}$ is state transition matrix for INS/GPS measurement equation.

$$\boldsymbol{W}_I = \begin{bmatrix} \omega_{gx} & \omega_{gy} & \omega_{gz} \end{bmatrix}^{\mathrm{T}} \tag{12}$$

$$\boldsymbol{W}_G = \begin{bmatrix} \omega_\varphi & \omega_\lambda \end{bmatrix}^{\mathrm{T}} \tag{13}$$

$$\boldsymbol{H}_{IG} = \begin{bmatrix} 1 & 0 & 0 & 0 & 0 & 0 & 0 & 0 & 0 & 0 & 0 & 0 & 0 & -1 & 0 \\ 0 & 1 & 0 & 0 & 0 & 0 & 0 & 0 & 0 & 0 & 0 & 0 & 0 & 0 & -1 \end{bmatrix} \tag{14}$$

Velocity integrated mode is used for INS/DVL sub filter, so the state equation and measurement equation are given by:

$$\begin{bmatrix} \dot{\boldsymbol{X}}_I \\ \dot{\boldsymbol{X}}_D \end{bmatrix} = \begin{bmatrix} \boldsymbol{F}_I & \boldsymbol{0} \\ \boldsymbol{0} & \boldsymbol{F}_D \end{bmatrix} \begin{bmatrix} \boldsymbol{X}_I \\ \boldsymbol{X}_D \end{bmatrix} + \begin{bmatrix} \boldsymbol{W}_I \\ \boldsymbol{W}_D \end{bmatrix} \tag{15}$$

$$\boldsymbol{Z}_{ID} = \begin{bmatrix} \boldsymbol{V}_{Ix} - \boldsymbol{V}_{Dx} \\ \boldsymbol{V}_{Iy} - \boldsymbol{V}_{Dy} \end{bmatrix} = \boldsymbol{H}_{ID} \begin{bmatrix} \boldsymbol{X}_I \\ \boldsymbol{X}_D \end{bmatrix} + \boldsymbol{V}_{ID} \tag{16}$$

Where $\boldsymbol{X}_D = \begin{bmatrix} \delta V_{Dx} & \delta V_{Dy} & \delta k \end{bmatrix}^{\mathrm{T}}$ is state variable of DVL velocity estimation error, $\delta V_{Dx}, \delta V_{Dy}$ are velocity error, δk is scale error. $\boldsymbol{F}_D$ is DVL state transition matrix:

$$\boldsymbol{F}_D = \mathrm{diag}(\frac{1}{\tau_{Dx}}, \frac{1}{\tau_{Dy}}, \frac{1}{\tau_k}) \tag{17}$$

Where $\tau_{Dx}, \tau_{Dy}, \tau_k$ are Markov correlation time, $\boldsymbol{W}_D$ is system noise matrix, ω_{Dx}, ω_{Dy} are driven white noise, $\boldsymbol{V}_{ID}$ is DVL measure noise matrix.

$$\boldsymbol{W}_G = \begin{bmatrix} \omega_{Dx} & \omega_{Dy} \end{bmatrix}^{\mathrm{T}} \tag{18}$$

$$\boldsymbol{H}_{ID} = \begin{bmatrix} 0 & 0 & 1 & 0 & 0 & 0 & -V_y & 0 & 0 & 0 & 0 & 0 & 0 & -1 & 0 & -V_x \\ 0 & 0 & 0 & 1 & 0 & 0 & V_x & 0 & 0 & 0 & 0 & 0 & 0 & 0 & -1 & -V_y \end{bmatrix} \tag{19}$$

6.2 Design for INS/GPS/DVL global filter

To make the integrated filter realizable for computer calculation, it is necessary to discretize the state equation and measurement equation mentioned above, and then we have:

$$\begin{cases} \boldsymbol{X}_k = \boldsymbol{\Phi}_{k,k-1} \boldsymbol{X}_k + \boldsymbol{\Gamma}_{k-1} \boldsymbol{W}_{k-1} \\ \boldsymbol{Z}_k = \boldsymbol{H}_k \boldsymbol{X}_k + \boldsymbol{V}_k \end{cases} \tag{20}$$

Assuming that the local estimations are unrelated, the global estimation can be expressed as:

$$\begin{cases} \hat{\boldsymbol{X}}_g = \boldsymbol{P}_g (\boldsymbol{P}_{11}^{-1} \hat{\boldsymbol{X}}_1 + \boldsymbol{P}_{22}^{-1} \hat{\boldsymbol{X}}_2) \\ \boldsymbol{P}_g = (\boldsymbol{P}_{11}^{-1} + \boldsymbol{P}_{22}^{-1})^{-1} \end{cases} \tag{21}$$

Local estimates ($\hat{\boldsymbol{X}}_1$, $\hat{\boldsymbol{X}}_2$) from the sub filters and their covariance matrix ($\boldsymbol{P}_1, \boldsymbol{P}_2$) participate in master filter algorithm, and the obtained results would integrate with master filter estimates to get the global optimal estimation. Besides, global estimate $\hat{\boldsymbol{X}}_e$ and the corresponding covariance matrix $\boldsymbol{P}_e$ are amplified to be $\beta_i^{-1} \boldsymbol{P}_g (\beta_i \le 1)$, being the feedback to sub filters, and estimates of sub filter are reset as:

$$\begin{cases} \hat{\boldsymbol{X}}_i = \hat{\boldsymbol{X}}_g \\ \boldsymbol{P}_{ii} = \beta_i^{-1} \boldsymbol{P}_g \end{cases} \tag{22}$$

7. Simulation

7.1 Simulation condition

(1) Initial latitude and longitude are $\varphi_0 = 30^\circ$ and $\lambda_0 = 120^\circ$ respectively; gyro constant drift is $0.01^\circ / \mathrm{h}$; head angel is 45°, and east velocity and north velocity are 5kn; simulation time is 20000*s*.

(2) INS/DVL/GPS integrated system is applied to calibration. After 4-hour system work, inertial system is calibrated by the gyro drift estimated and system error information.

(3) On the two conditions of GPS information with no fault and slope failure, calibration simulation is implemented. Slope of the slope failure is set as mentioned in Section 3.3.

7.2 Simulation results

On the two conditions of GPS information with no fault and slope failure, the estimated results for east gyro drift and azimuth gyro are given in Figure 7, and the latitude and longitude information is shown as figure 8.

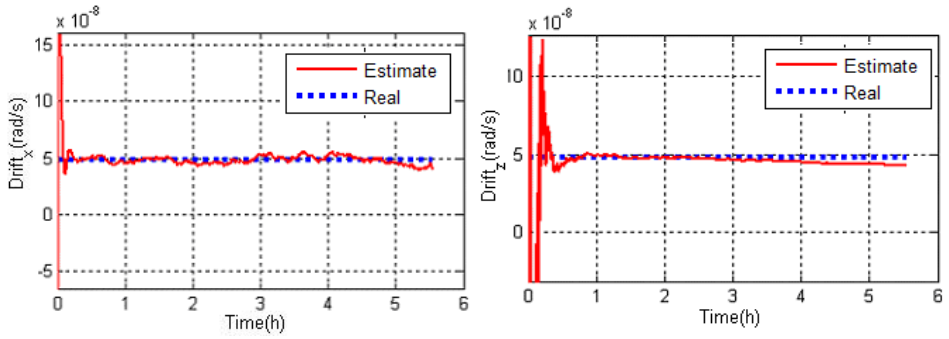

(a) The drift estimation results when GPS is without faults

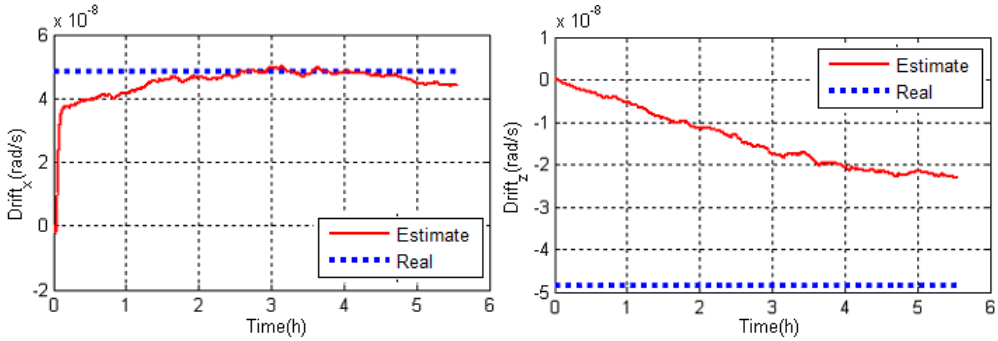

(b) The drift estimation results when GPS have slope faults

Figure.7 Gyro drifts estimation result

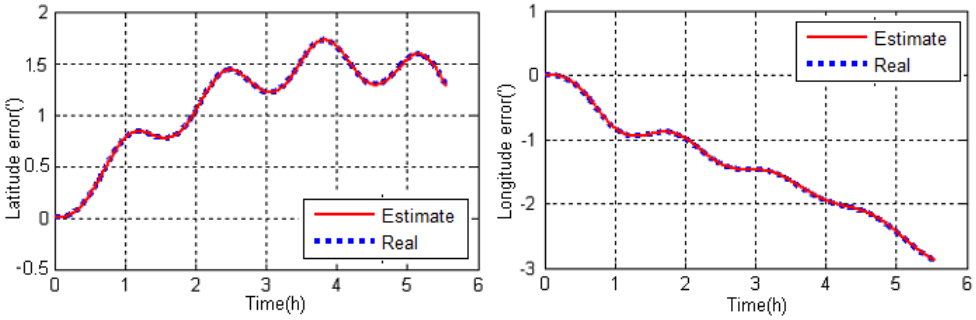

(a) The positioning result when GPS is without faults

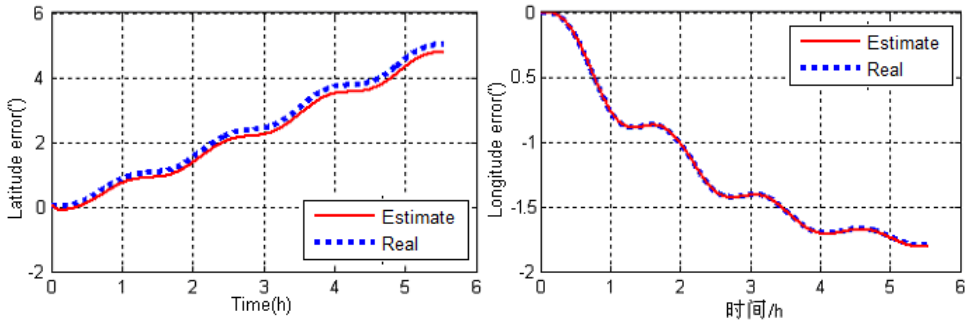

(b) The positioning results when GPS have slope faults

Figure.8 Positioning estimation results

It can be seen from the simulation curves on the no-faults condition, inertial navigation system gyro drifts and position information can be estimated well by the INS/DVL/GPS integrated calibration, especially the estimation accuracy for east gyro drift can be up to 90%. Besides, according to the

simulation results when there is slope fault, influenced by the fault information, federated filter can not obtain the position observation information, leading to the decrease of gyro drift estimation. In addition, through the detection and isolation for faults, the single system fault will have no effects on SINS/DVL sub filter because the GPS with abnormal output is isolated, but the federated filter change to be composed of SINS/DVL sub filter equivalently, which cause the slightly decrease for the position estimation comparing with the situation without GPS faults.

8. Simulation

Aiming at the problems that INS calibration accuracy will be affected because sensor fault detection algorithm is insensitive, large-delay and can not distinguished faults type, a developed fault-tolerant federated filtering algorithm based on wavelet singular value detection have been proposed in this paper. Through multi-sensor federated filtering, the single navigation sensor fault can not affect the performance of the entire system. Based on wavelet modulus maxima, the navigation sensor fault detection method has high sensitivity to detection for navigation soft faults, and the fault type can be distinguished through the Lipschitz exponent on fault point. In order to provide effective information for the fault isolation and restoration of sensor, multi-sensor fault-tolerant integrated navigation system can be adopted, and the reliability of system can be improved. Simulation results show that the method proposed is effective and has important practical significance for engineering application.

Acknowledgment

Funding for this work was provided by the National Nature Science Foundation of China under grant No. 61374007 and No. 61104036, and the Fundamental Research Funds for the Central Universities under the grant of HEUCFX41309. The authors would like to thank all the editors and anonymous reviewers for improving this article.

References

[1] G.T. Schmidt, “INS/GPS Technology Trends,” *Advances in Navigation Sensors and Integration Technology*, 2011.

[2] M.L. Cao , P.Y. Cui, “Information fusion technology of INS/GPS navigation system based on wavelet fault detection,” *Journal of Astronautics*, vol.30, no.5, pp.1885-1887, 2009.

[3] Z.X. Zhang, F. Zhang, “Advanced residual chi-square test method based on state propagator,” *Journal of Chinese Inertial Technology*, vol.17, no.1, pp.107-108, 2009.

[4] D.E. Gaylor, “GPS/INS Kalman filter design for spacecraft operating in the proximity of the inter national space station,” *American Institute of Aeronautics and Astronautics Guidance, Navigation, and Control Conference*, Reston, VA, USA, August 11-14, 2003.

[5] F.J. He, “Research on the detection technology for sensors faults,” *Science Technology and Engineering*, vol.10, no.26, pp.6481-6485, 2010.

[6] Qu Zhihong, "Information fusion application in INS/GPS/DVS integrated navigation system," *Electronic Measurement Technology*, vol.30, no.90, pp.187-190, 2007.

[7] W.L. Hwang and S. Mallat, "Singularities and noise discrimination with wavelets," *Acoustics, Speech, and Signal Processing Conference*, San Francisco, USA, Mar 23-26, pp.377-380, 1992.

[8] Y.K Sun, Wavelet Analysis and Its Application, China Machine Press, 2004: 199-205.

[9] P. Shen, H.M. Zhang, "The research of fault detection technique based on wavelet analysis in integrated navigation system," *Chinese Journal of Scientific Instrument*, vol.30, no.10, pp.80-81, 2009.

[10] Mallat, S.F Zhong, "Characterization of signals from multi-scale edges," *IEEE Transactions on Pattern Analysis and Machine Intelligence*, vol.14, no.7, pp.710-713, 1992.

[11]S.H Xu, J.H. Wu, and Z.Q. Hu, "Research on wavelet transform method for the fault-detection of the integrated navigation system," *Journal of Astronautics*, vol.24, no.1, pp.111-112, 2003.

[12]S.S. Hu, C. Zhou, and W.L. Hu, "A new structure fault detection method based on wavelet singularity," *Journal of Applied Sciences*, vol.18, no.3, pp.199-201, 2000.

[13] Y. Liu, Y. Li, and J.T. Xu, "Real-time filtering based on multiple algorithm fusion for fiber optic gyro," *Acta Photonica Sinica*, vol.39, no.6, pp.1116-1117, 2010.

[14]Y.N. Wang, X. Deng, and W. Zhao, "Application of Fuzzy Adaptive Kalman Filter Based on Weighted Matrix in Integrated Navigation System," *Journal of Chinese Inertial Technology*, vol.16, no.3, pp.334-338, 2008.